Hypersonic flow over axially symmetric spiked bodies

By D. J. MAULL
Department of Aeronautics, Imperial College, London University*

(Received 6 January 1960)

An investigation has been made of the flow over axisymmetric spiked bodies at a Mach number of 6·8. For some ranges of the ratio of spike length to body diameter the flow was found to be unsteady. The effect of the shape of the body nose on this unsteadiness was investigated and an explanation of the mechanism of the oscillation is given.

1. Introduction

The supersonic flow around axially symmetric blunt bodies is characterized by the presence of a strong bow shock wave standing away from the nose of the body. The presence of this shock wave results in a high drag coefficient compared with that of a pointed body with an attached nose shock wave.

It has been shown by Eggers & Allen (1958) that for a body re-entering the earth's atmosphere at a high supersonic speed, it is advisable, to minimize heating effects, to have a body whose nose radius and drag coefficient are high. However, for motion through the earth's atmosphere at take off, it is necessary to have a body with a low drag coefficient to make the best use of the thrust of the propulsive system. It would therefore be an advantage for a body such as a re-entry missile to be equipped with some form of variable drag device.

The object of this investigation has been to study the flow over such a device, namely a blunt body equipped with a nose spike (figure 1). The tests were carried out in the Imperial College hypersonic gun tunnel at a Mach number of 6·8 and a Reynolds number of $0{\cdot}17 \times 10^6$/in.

2. Experimental facility and models

The Imperial College hypersonic gun tunnel has been described by Stollery, Belcher & Maull (1960). For this series of experiments the driving gas was air at approximately 600 p.s.i. and the working gas was air at initially room temperature and pressure. The nozzle used gave a Mach number of approximately 6·8 and the total running time of the steady flow was approximately 300 msec.

Five different model configurations were used. These were a plain flat-ended cylinder and four models having rounded nose shoulders with radii one-eighth, one-quarter, three-eighths and one-half of the cylindrical body diameter (figure 1).

The models were made of brass, the cylindrical portion being $\frac{1}{2}$ in. in diameter. The spike was a commercial sewing needle 0·030 in. in diameter which screwed

* Now at Engineering Laboratory, University of Cambridge.

into the nose of the body. The models were mounted at zero angle of incidence on a support in the working section.

Both schlieren and shadow photographs were taken of the flow, the schlieren arrangement being of the double pass type. A single-spark light source of duration approximately $1\,\mu s$ was used for most studies although for some configurations a multiple spark source (Cranz-Schardin) was used. This gave a series

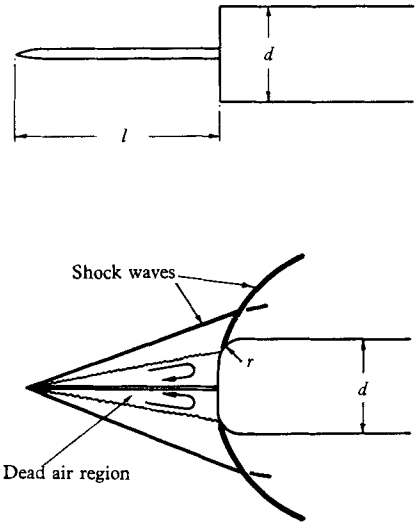

FIGURE 1. Spiked blunt-nosed bodies.

of eight sparks, which, by suitable optical arrangements, could be photographed on one half plate. The time interval between the sparks was variable down to $5\,\mu s$.

A high-speed ciné camera was also used to investigate the flow using a constant intensity mercury-vapour light source. The cameras and the spark sources were triggered electronically by picking up the noise of the tunnel start on a microphone, and passing this pulse via a delay circuit to the apparatus.

3. Results

3.1 *Test programme*

For each body, schlieren photographs of the flow were taken as the ratio of the spike length l to the body diameter d was varied over the range $0 \leqslant l/d \leqslant 4$. It was found that for $l/d > 4$ the spike vibrated and investigations at these spike lengths were not carried out. When unsteady flow was suspected a series of spark photographs was taken. Initially a high-speed ciné picture of some of the oscillations was taken but the oscillations were of too high a frequency to be picked up by the ciné camera.

3.2. *The oscillatory flow*

It was found that there was an oscillation of the flow around the flat-nosed body with spike lengths in the range $0{\cdot}25 < l/d \leqslant 2{\cdot}5$. The lower limit of this range was difficult to determine, but it appears that oscillation began when the spike

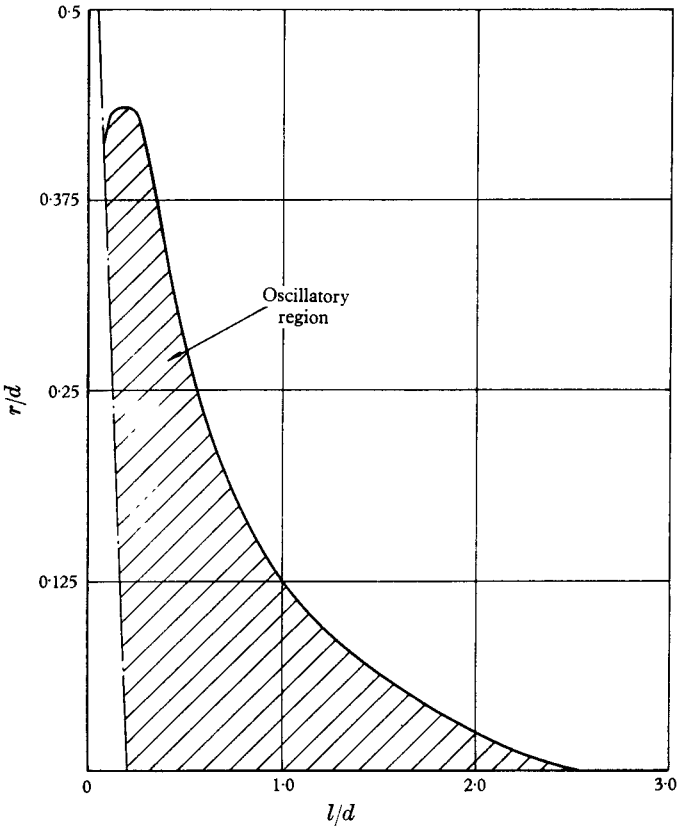

FIGURE 3. The effect of shoulder radius on the oscillatory region.

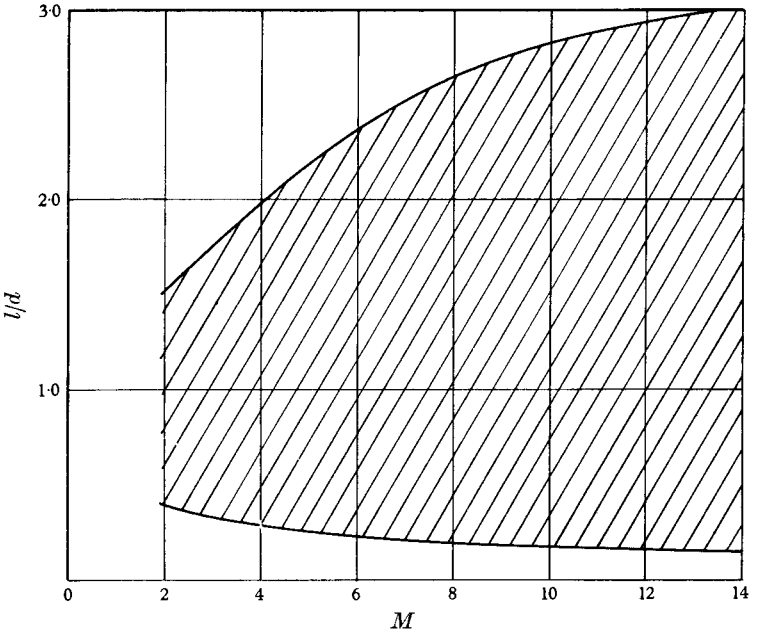

FIGURE 4. The oscillatory range against Mach number for flat-ended cylinders ($r/d = 0$).

protruded through the bow shock wave of the body. A typical spark shadowgraph photograph of the unsteady flow is shown in figure 2 (plate 1). By using the Cranz-Schardin spark source it was possible to determine the spike length required for oscillation to cease. By comparing a series of photographs taken with the Cranz-Schardin camera with the sparks set at $10\,\mu$s intervals the frequency of the oscillation was found to be approximately 2×10^4 c/s.

The flow around the spiked hemispherically nosed body was steady for all spike lengths, but all the bodies whose shoulder radius was less than half the diameter of the cylindrical portion of the body had ranges of spike lengths for which oscillation occurred. It is thus possible to draw the range of spike length for which oscillation occurred against shoulder radius (figure 3).

The investigations of Mair (1952) and Bogdonoff & Vas (1959) showed oscillation of the flow pattern for the flat-nosed cylinder with a spike at different Mach numbers and hence a graph of the oscillatory range against Mach number may be drawn for this configuration (figure 4). It should be noted that the experiments of Bogdonoff & Vas were performed in helium.

4. Discussion

A thorough investigation of separated flows has been reported by Chapman, Kuehn & Larson (1957) for the two-dimensional case of flow up and down steps. The only theoretical investigation of the problem of flow separation caused by a spike on a blunt body is by Moeckel (1951*a*), who used a simple theoretical model in which the separated shear layer re-attaches tangentially to the nose of the body. The assumption of tangential re-attachment is found to be in error in both this investigation and subsequent work by Moeckel (1951*b*). The three-dimensional problem may be subdivided into two parts, the separation of the boundary layer on the spike and the re-attachment of the separated shear layer.

4.1. *Shock-induced separation*

A boundary layer will be separated by a sufficiently strong shock wave which is either generated externally by another body in the flow field or by some influence of the body itself. Thus the boundary layer on the nose spike of a blunt body will separate initially under the influence of the nearly normal bow shock wave of the body if the spike protrudes through this shock wave. This separated layer will re-attach on the face of the body enclosing an approximately conical region between itself and the face. This region which will contain some circulatory flow will, in the text, be called the 'dead air region'. A conical shock wave will be required to turn the main flow past this dead air region. This conical shock wave may still be stronger than is required to separate the boundary layer at this point on the spike and will influence the boundary layer upstream causing further separation. If the separated layer still re-attaches on the face of the body the resulting conical shock wave will have a smaller half-cone angle and its strength, as measured by the pressure ratio across it, will decrease.

The pressure ratio, which the boundary layer can withstand without separation, increases as the distance from the nose of the spike decreases, and since the

pressure ratio across the conical shock wave decreases as the distance from the spike nose decreases an equilibrium position must be reached where the boundary layer will just separate.

The pressure ratio that will just cause separation is thus a function of Mach number and Reynolds number based on the distance of the separation point from the spike nose. Thus the angle that the separated layer makes with the spike axis is also a function of these two parameters.

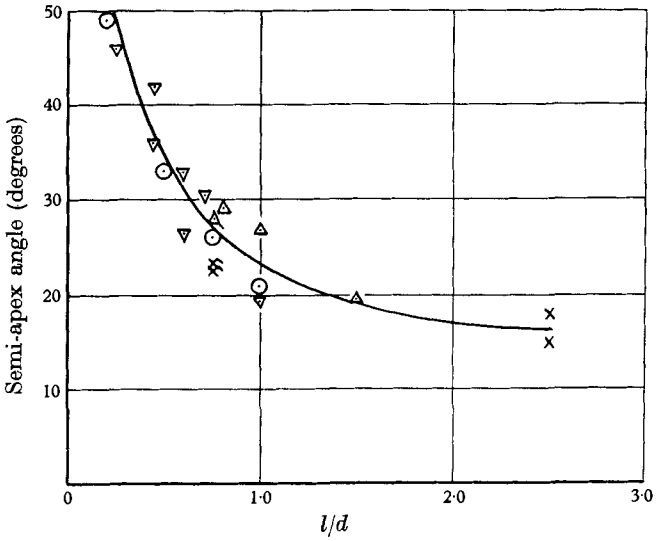

FIGURE 5. The semi-apex angle of the conical shock wave about the dead air region against l/d. The symbols indicate the different shoulder radii. ×, $r/d = 0$; △, $r/d = \frac{1}{4}$; ▽, $r/d = \frac{3}{8}$; ⊙, $r/d = \frac{1}{2}$. The flagged symbols indicate unsteady flow.

At the beginning of a cycle of the oscillatory flow under consideration the separation point appears to be very close to the nose of the spike and it is not possible to measure accurately its position. A plot of the measured shock half-cone angle against spike length (figure 5) shows that the shock angle decreases with increased spike length, indicating a useful reduction in drag as found by Mair and by Bogdonoff & Vas. The majority of these measured angles are from flow photographs of the steady conditions, but some are from unsteady flow photographs where the oscillation cycle is just beginning and the dead air region is approximately conical with separation near the spike tip.

It is apparent from figure 5 that the shock angle, to a first approximation, is a function of the spike length rather than the shape of the nose of the body. In figure 6 the apex semi-angle of the separated layer as calculated from the shock angles of figure 5 is plotted against spike length.

4.2. *Re-attachment process*

The analysis of the re-attachemnt process by Chapman *et al.* assumes laminar two-dimensional flow. It is not possible to use their results for the three-dimensional re-attachment under consideration, but the basis of their analysis serves as a guide to the mechanism of re-attachment.

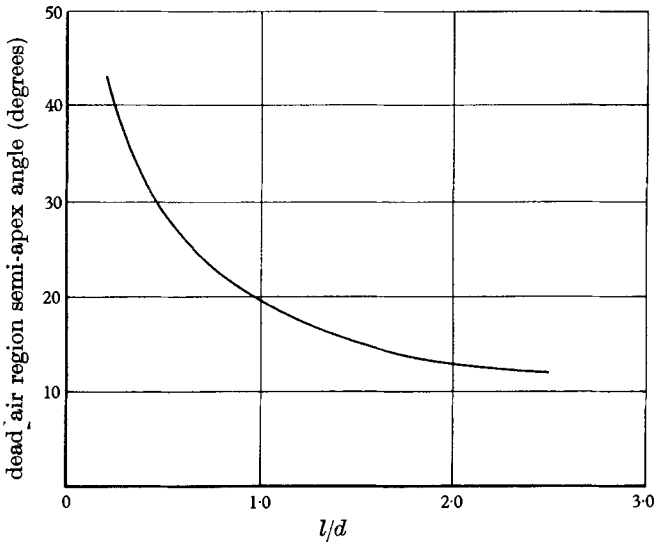

FIGURE 6. The semi-apex angle of the dead air region.

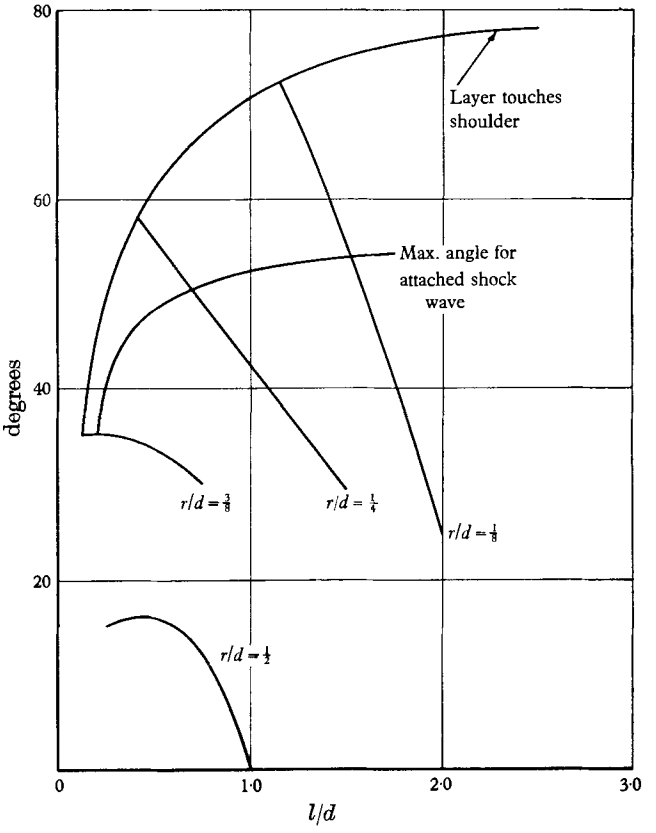

FIGURE 7. The angle between the separated layer and the body at the point of re-attachment against l/d. For $r/d = 0$ the separated layer touches the shoulder at the point shown.

The separated shear layer scavenges air from the dead air region and for equilibrium the mass of air scavenged must equal the mass reversed by a pressure gradient at the re-attachment point. From Chapman *et al.* the pressure at re-attachment that the separated layer can support under these equilibrium conditions is a function of the Mach number outside the shear layer. It is thus a function of the free-stream Mach number and the angle that the separated layer makes with the spike axis.

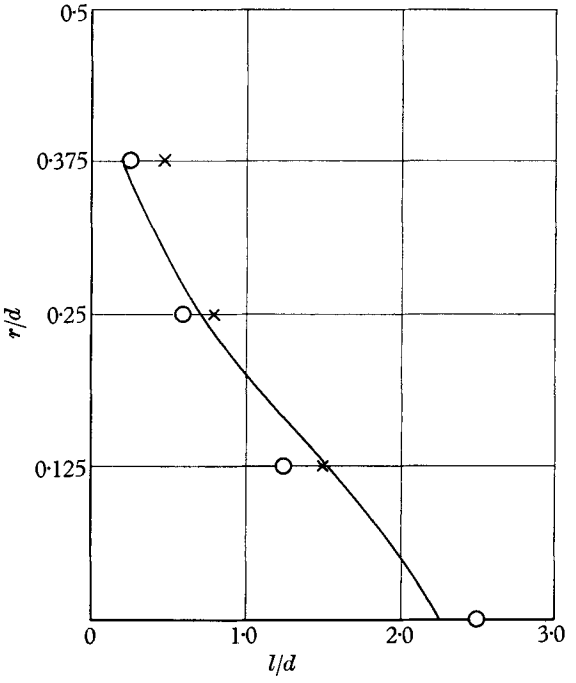

FIGURE 8. Comparison of the theoretical boundary of the oscillatory region with experimental results. ○, oscillatory flow; ×, steady flow.

If the separated layer re-attaches on the nose of the body non-tangentially, there must be an oblique shock at the re-attachment point to turn the supersonic flow just outside the layer up the nose of the body. If the pressure ratio across this oblique shock is such that the mass of air reversed at the re-attachment point balances the mass of air scavenged from the dead air region by the shear layer, then there will be steady flow.

From the measured angle between the separated layer and the spike axis (figure 6) it is possible to calculate, for the different configurations, the angle that the separated layer makes with the tangent to the body at the point of impingement (figure 7). It is also possible to calculate the maximum conical flow deflexion angle for the local Mach number prevailing on the conical surface of the separated region. If the angle through which the flow must be turned is greater than this, a detached shock wave is required, standing off from the point of impingement.

It is very unlikely that the separated layer can support this detached shock wave without the majority of the shear layer being reversed back into the dead

air region, and this shock pattern is certainly unstable. The lengths of spike to give this condition agree quite closely with the bounds of the observed oscillatory range (figure 8).

It should be noted that the maximum turning angle used in this analysis is that given by conical flow graphs whereas the maximum angle through which flow on the surface of a cone may be turned is theoretically given by the two-dimensional shock equations.

4.3. *Mechanism of the oscillation*

Figure 9 (plate 2) shows five spark shadowgraph photographs of the oscillatory flow about the flat-ended cylinder at a spike length three-quarters of the body diameter. The cycle starts with the boundary layer on the spike separating near the nose forming an approximately conical dead air region, which if continued to the face of the body would strike it well below the shoulder (figure 9*a*). To turn the flow just outside the separated layer up the nose of the body a detached shock wave is required. The pressure ratio across this shock and the area behind the shock through which air may be reversed into the dead air region are certainly too great for equilibrium to occur with the mass of air scavenged from the dead air region before the shock. Thus a non-equilibrium condition occurs with air flowing into the dead air region down the body nose. This enlarges the dead air region forming a nearly normal shock wave at the spike tip (figure 9*b*) which grows and replaces the conical shock wave. In figure 9*b* this growth has only just started.

The flow into the dead air region goes along the spike and the shock pattern should resemble the pattern produced by a jet of air from the body injected against the main stream. Figure 10 (plate 2) shows this flow pattern.

The strong shock wave grows from the spike tip as more air is fed into the dead air region. As it grows the intersection with the bow shock wave of the body moves out towards the shoulder of the body (figure 9*c*). The dead air region by this time is not conical but blunt in shape, with the re-attachment region moving up the face of the body. As the dead air region broadens, the angle through which the external flow must be turned at the end of it to pass round the nose decreases and the presssure ratio across the shock which turns it decreases. Thus the feeding of air into the dead air region stops. Air is now fed from the region out past the shoulder; the dead air region collapses and the shock wave which was at the spike tip moves towards the body (figure 9*d*) and grows weaker (compare figure 9*c* and *d*). As this shock wave moves downstream along the spike, separation again occurs at the spike tip with a conical shock wave formed (figure 9*e*). When the excess air in the dead air region has escaped and the strong shock wave originally at the spike tip has become the bow shock wave of the body the cycle begins again.

An interesting feature of figure 9*b* are the vortex sheets at the intersection of the conical shock wave and the bow shock wave. They are shown by Mair to be quite tightly closed. The strong shock wave near the body on figure 9*e* only appeared on one photograph in twenty of this configuration and occurs at the end of the period of the dead air region collapsing. This strong shock wave is probably

moving slowly upstream, and will merge with the bow shock wave originally at the spike tip to form the initial bow shock wave for the main body.

Lengthening the spike has the effect of moving the point of re-attachment of the separated layer up the nose of the body towards the shoulder. When the re-attachment point is at the shoulder of the flat-faced cylinder the supersonic flow just outside the separated layer can turn the corner through an expansion, and there will be no feed-back of air into the dead air region and no oscillation.

For bodies with rounded shoulders it is possible for the flow just outside the separated layer to be turned up by the nose by an oblique shock wave when the re-attachment point is far enough out on the rounded part of the nose. There will be a re-attachment point where the pressure ratio across the oblique shock wave is just sufficient for equilibrium of the dead air region and no oscillation occurs. This condition is shown in figure 11 (plate 1).

4.4. *Frequency of the oscillation*

The frequency of the oscillation as measured from the Cranz–Schardin photographs was about 2×10^4 c/s. A non-dimensional frequency may be defined as fd/u, where f is the measured frequency, d the body diameter and u the free-stream velocity. For the results in this report, this gives a non-dimensional frequency of 0·23. The results of Mair give a non-dimensional frequency of 0·15 at a Mach number of 1·96.

5. Conclusions

The investigation has shown that while fitting a spike to the nose of a blunt body may reduce the drag coefficient, it may in some cases cause a rapid fluctuation of the flow pattern and thus produce an unsteady drag coefficient.

The practical use of such a device must therefore be limited to bodies which do not exhibit these changes in flow pattern. The length of the spike will be determined by structural considerations and the shorter the spike the more the nose shape must tend towards a hemisphere for steady flow. It is also thought that bodies whose noses are not so blunt as hemispheres, i.e. ellipsoids of revolution, would also be stable with nose spikes.

REFERENCES

Bogdonoff, S. M. & Vas, E. 1959 *J. Aero./Space Sci.* **26**, 65.
Chapman, D. R., Kuehn, D. M., & Larson, H. K. 1957 *NACA TN* 3869.
Eggers, A. J. & Allen, M. J. 1958 *NACA Rep.* 1381.
Mair, W. A. 1952 *Phil. Mag.* **43**, 695.
Moeckel, W. E. 1951*a* *NACA TN* 2418.
Moeckel, W. E. 1951*b* *NACA RM* E51I25.
Stollery, J., Belcher, B. & Maull, D. J. 1960 *J. R. Aero. Soc.* **64**, 24.

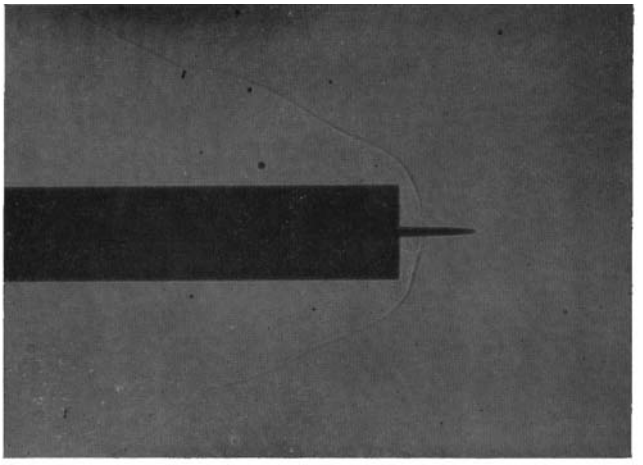

FIGURE 2 (plate 1). A typical photograph of the unsteady flow.

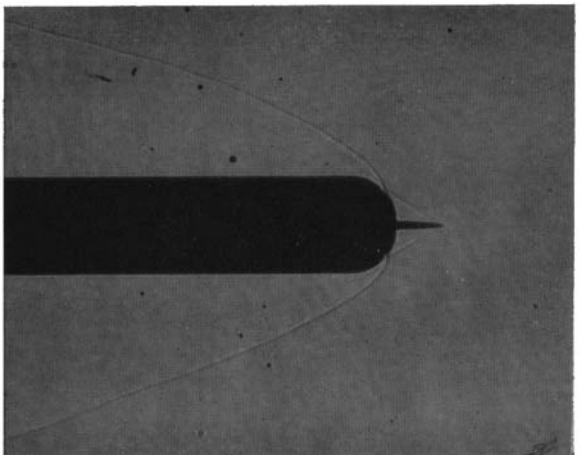

FIGURE 11 (plate 1). Steady conical separation from a spike on a hemispherically nosed body.

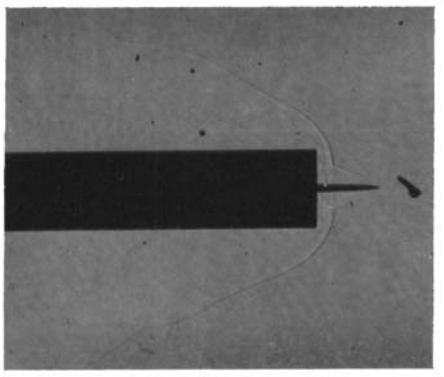

a

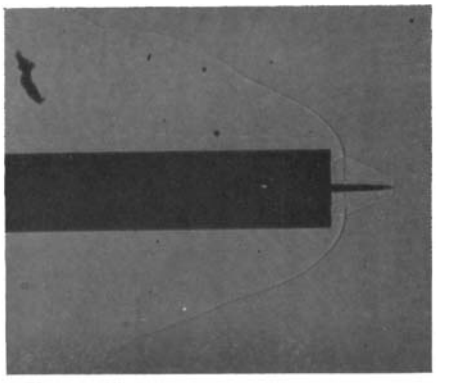

b

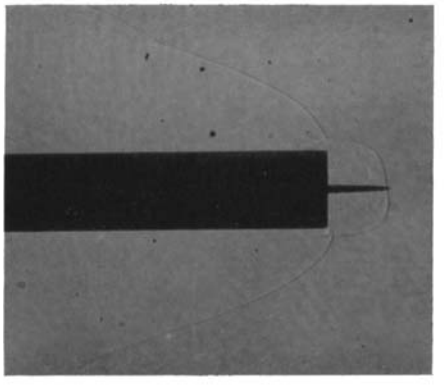

c

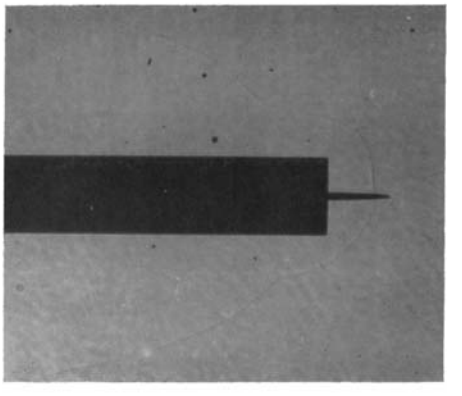

d

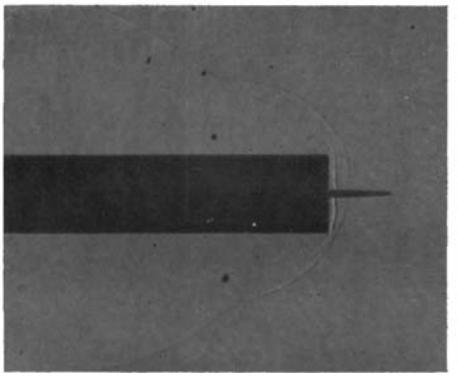

e

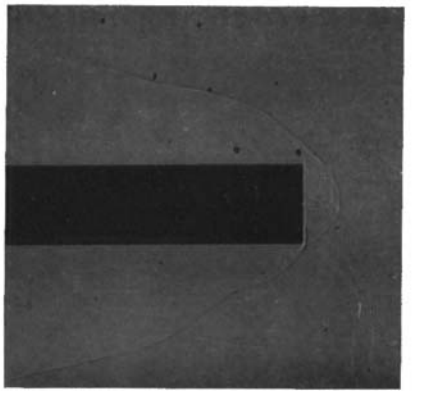

FIGURE 10

FIGURE 9 (plate 2). Phases of the oscillation for the spiked body with $l/d = 0{\cdot}75$, $r/d = 0$.

FIGURE 10 (plate 2). The shock pattern produced by air blowing out of the front of a flat-ended cylinder.